

# No $^{182}\text{W}$ excess in the Ontong Java Plateau source

Thomas S. Kruijer<sup>1,2,\*</sup>, Thorsten Kleine<sup>1</sup>

<sup>1</sup>Institut für Planetologie, University of Münster, Wilhelm-Klemm-Strasse 10, 48149 Münster,  
Germany.

<sup>2</sup>Nuclear and Chemical Sciences Division, Lawrence Livermore National Laboratory, 7000 East  
Avenue (L-231), Livermore, CA 94550, USA

Revised manuscript submitted to *Chemical Geology*

Version: 14 March 2018

Main text: 5418 words

Abstract: 335 words

1 table

6 figures

1 Supplementary table

1 Supplementary figure

\*Corresponding author:

E-mail: [kruijer1@llnl.gov](mailto:kruijer1@llnl.gov)

Phone: +1-925-42-29262

## ABSTRACT

31 Small-scale W isotope variations in ancient and modern terrestrial rocks provide insights into Earth's  
32 accretion and early differentiation history as well as the long-term evolution of the Earth's mantle.  
33 Tungsten isotope studies on such rocks have exploited advances in mass spectrometry, both NTIMS  
34 and MC-ICPMS, which now permit the determination of W isotope ratios at unprecedented precision.  
35 While W isotope studies performed in different labs by MC-ICPMS and NTIMS generally exhibit  
36 excellent agreement, obtaining accurate W isotope data at this level of precision remains analytically  
37 challenging. For example, a recent NTIMS study reported a relatively large, +24 ppm excess in  
38  $^{182}\text{W}/^{184}\text{W}$  for a Phanerozoic sample from the Ontong Java Plateau (OJP), but no such  $^{182}\text{W}/^{184}\text{W}$   
39 anomaly was found in another study by MC-ICPMS. The present study aims to resolve the  
40 discrepancy between these two previous studies, and more generally to evaluate the agreement  
41 between different recent W isotope studies by NTIMS and MC-ICPMS. To this end, we report new W  
42 isotope data for OJP drill core samples obtained by MC-ICPMS. The OJP samples analyzed here  
43 exhibit no resolvable  $^{182}\text{W}/^{184}\text{W}$  excess relative to the standards and most terrestrial rocks. Moreover,  
44 the OJP samples as well as the terrestrial rock standards analyzed here exhibit small but variable W  
45 isotope variations for ratios involving  $^{183}\text{W}$ , producing coupled variations in both 'radiogenic' (*i.e.*,  
46  $^{182}\text{W}/^{183}\text{W}$ ) and 'non-radiogenic' (*i.e.*,  $^{183}\text{W}/^{184}\text{W}$ ) ratios. These W isotope variations are analytical in  
47 origin, induced during sample preparation, and very likely caused by a nuclear field shift isotope  
48 fractionation affecting primarily the odd isotope ( $^{183}\text{W}$ ). The recently reported  $^{182}\text{W}$  excess for an OJP  
49 sample may result from this nuclear field shift effect, as the NTIMS analyses had to rely on a double  
50 normalization involving the  $^{183}\text{W}/^{184}\text{W}$  ratio. More generally, these results demonstrate that using  
51  $^{183}\text{W}$  data from any MC-ICPMS or NTIMS study requires a careful quantification of any potential  
52 analytical  $^{183}\text{W}$  effect. Nevertheless, once such effects are taken into account, then both  $^{182}\text{W}/^{184}\text{W}$  and  
53  $^{183}\text{W}/^{184}\text{W}$  can accurately be determined to a very high level of precision.

54

55

56 **Keywords:** Archean rocks, Hf-W system, MC-ICPMS, NTIMS, mantle differentiation, late accretion

57

## 58 1. Introduction

59 The short-lived  $^{182}\text{Hf}$ - $^{182}\text{W}$  system (half-life: 8.9 Ma) has been widely used as a chronometer for  
60 dating early solar system processes including planetary core formation (see e.g., Jacobsen, 2005;  
61 Kleine et al., 2009; Kleine and Walker, 2017). Nevertheless, through recent advances in measurement  
62 techniques the Hf-W system is now also used to study the evolution of the Earth's mantle. In  
63 particular, analytical improvements in isotope ratio mass spectrometry have enabled the resolution of  
64  $^{182}\text{W}/^{184}\text{W}$  measurements on the order of ~5-10 ppm (2s.d.). Such precise W isotope measurements  
65 are performed either using multi-collector inductively coupled plasma mass spectrometry (MC-  
66 ICPMS; e.g., Kruijjer et al., 2012; Willbold et al., 2011) or negative thermal ionization mass  
67 spectrometry (N-TIMS; Archer et al., 2017; Touboul and Walker, 2011). This improvement in  
68 measurement precision has provided new insights in the earliest history of the silicate Earth. For  
69 instance, Willbold et al. (2011) demonstrated that Archean rocks from the ~3.8 Ga Isua Supracrustal  
70 Belt exhibit small ~10-15 ppm excesses in  $\mu^{182}\text{W}$  relative to the present-day BSE (where  $\mu^{182}\text{W}$  is the  
71 parts-per-million deviation of  $^{182}\text{W}/^{184}\text{W}$  from the ratio of terrestrial standards). Moreover, Touboul et  
72 al. (2012) found W isotope anomalies of similar magnitude in ~2.8 Ga Kostomuska komatiites.

73 Subsequent studies have identified similar small-scale  $\mu^{182}\text{W}$  anomalies in several suites of Hadean to  
74 Archean terrestrial rocks with a total range in  $\mu^{182}\text{W}$  between *ca.*  $-8$  and  $+20$  (Dale et al., 2017; Liu et  
75 al., 2016; Puchtel et al., 2016; Rizo et al., 2016b; Touboul et al., 2014, 2012, Willbold et al., 2015,  
76 2011), although the data exhibit a preponderance of  $\mu^{182}\text{W}$  values between  $+10$  and  $+15$  ppm. More  
77 recently,  $^{182}\text{W}$  heterogeneities have also been reported for some Phanerozoic rocks, including samples  
78 from the Baffin Bay locale (60 Ma) and the Ontong Java Plateau (120 Ma) (Rizo et al., 2016a), as  
79 well as ocean island basalts from Hawaii, Samoa, and Iceland (Mundl et al., 2017). The existence of  
80  $\mu^{182}\text{W}$  anomalies in these young rocks implies that isotopically distinct mantle domains have survived  
81 until the present-day, and this has therefore been taken as evidence that the mantle has not completely  
82 mixed over geological history. The Ontong Java Plateau (OJP) in the western Pacific Ocean is the  
83 largest known volcanic province on Earth (Neal et al., 1997) and has geochemical characteristics that  
84 are consistent with a relatively primitive mantle source (Jackson et al., 2011), although this remains  
85 debated (Day, 2017).

86 There is considerable debate regarding the origin of the  $\mu^{182}\text{W}$  anomalies. They have been  
87 interpreted to reflect (i) late accretion of on average chondritic (*i.e.*,  $^{182}\text{W}$ -depleted) material following  
88 core formation and extinction of  $^{182}\text{Hf}$  (*e.g.*, Willbold et al., 2011, 2015; Dale et al., 2017), (ii) early  
89 silicate mantle differentiation processes within the lifetime of  $^{182}\text{Hf}$  (*e.g.*, Touboul et al., 2012; Rizo et  
90 al., 2016b), and (iii) early (incomplete) metal-silicate separation within the mantle (*e.g.*, Touboul et  
91 al., 2014; Rizo et al., 2016a; Mundl et al., 2017). Note that  $\mu^{182}\text{W}$  anomalies due to early  
92 differentiation would have to be generated within the lifetime of  $^{182}\text{Hf}$ , *i.e.*, very likely prior to the  
93 Moon forming impact. By contrast,  $\mu^{182}\text{W}$  anomalies due to late accretion would have been produced  
94 after the formation of the Moon (Touboul et al., 2007, 2015; Kruijer et al., 2015, 2017). Thus,  
95 identifying the origin of  $\mu^{182}\text{W}$  heterogeneities in Earth's mantle is essential for assessing whether  
96 signatures of early differentiation processes predating the formation of the Moon have been preserved.

97 One problem with the identification of  $\mu^{182}\text{W}$  anomalies in terrestrial samples is that these  
98 anomalies are very small and are at the edge of the analytical resolution of current mass spectrometric  
99 techniques. This issue becomes apparent when high-precision  $^{182}\text{W}$  data for some of the same samples  
100 analyzed in different laboratories and by different techniques are compared. For instance, for one OJP  
101 drill core sample (192-1187A-009R-04W), Rizo et al. (2016a), using NTIMS, reported one of the  
102 largest  $\mu^{182}\text{W}$  excesses measured so far for terrestrial samples ( $\mu^{182}\text{W} = +24 \pm 5$ ). However, Willbold  
103 et al. (2011), using MC-ICPMS, found no such  $\mu^{182}\text{W}$  excess in another OJP sample from the same  
104 drill core ( $\mu^{182}\text{W} = -7 \pm 6$  ppm; 192-1187A-006R-06W). In the same study, Rizo et al. (2016a) also  
105 reported an even larger  $\mu^{182}\text{W}$  excess of  $+48 \pm 5$  ppm for samples from Baffin Bay. Understanding the  
106 cause of the disparate results for the OJP samples is important not only for understanding as to  
107 whether there is a  $\mu^{182}\text{W}$  anomaly in these samples, but also because the  $\mu^{182}\text{W}$  excesses for OJP and  
108 Baffin Bay reported by Rizo et al. (2016a) would be difficult to account for by late accretion. Thus, if  
109 these  $^{182}\text{W}$  excesses are confirmed, then this would be strong evidence that vestiges of Earth's earliest  
110 differentiation, predating the formation of the Moon, have been preserved in Earth's mantle until the  
111 present day.

112 The objectives of the present study are to evaluate and document the accuracy and  
113 reproducibility of W isotope measurements by MC-ICPMS, compare this to the NTIMS technique,  
114 and to ultimately assess whether there is a  $\mu^{182}\text{W}$  anomaly in the OJP source. To this end new  $\mu^{182}\text{W}$   
115 data for Ontong Java samples as well as for terrestrial reference materials (BHVO-2, BCR-2) are  
116 reported.

## 117 2. Samples and analytical methods

### 118 2.1. Sample preparation and chemical separation

119 For this study, different digestions (~0.5 g) of the geological reference material BHVO-2 was  
120 analyzed several times, and the results for these two samples are presented together with BHVO-2 and  
121 BCR-2 data obtained in the Münster laboratory since 2012. For the OJP samples, two drill core  
122 samples, provided by the Ocean Drilling Program (ODP), were selected for high-precision W isotope  
123 analyses (192-1187A-04W 15-17; 192-1187A-04W 118.5-120). These samples are from the same  
124 drill core section (Site 1187; Core A) and are the exact same lithology and lava flow as the sample  
125 analyzed by Rizo et al. (2016a) (192-1187A-04W 125-138). Moreover, one of the two samples from  
126 this study (192-1187A-04W 118.5-120) was collected only a few cm apart from the sample analyzed  
127 by Rizo et al. (2016a) (Fig. S1). Of note, the total amount of OJP sample used here for a high-  
128 precision W isotope measurement by MC-ICPMS is ~9.5 g, significantly smaller than the ~44 g  
129 required for a NTIMS measurement of similar precision (Rizo et al., 2016a).

130 The analytical techniques for sample digestion, chemical separation of W, and W isotope ratio  
131 measurements by MC-ICPMS are based on methods described in several prior studies from the  
132 Münster laboratory (e.g., Budde et al., 2016; Kruijer et al., 2015, 2014). The OJP samples were  
133 received as rock fragments and visually inspected upon arrival. No obvious signs of alteration were  
134 observed and the samples most likely stem from the interior parts of the drill core. It should be noted  
135 already here that, because all investigated OJP samples exhibit very low and uniform W  
136 concentrations (Section 5-6; Table 1), significant W contamination from W-enriched source (e.g., the  
137 drill bit) can effectively be ruled out. The OJP samples were cleaned with abrasive paper, then  
138 ultrasonically cleaned and rinsed with ethanol, and finally crushed and ground to a fine powder in an  
139 agate mortar. Powders of terrestrial rock standards and OJP samples were split into ~2 g powder  
140 fractions and then digested in 40 ml concentrated HF–HNO<sub>3</sub> at ~120-130 °C in 60 ml Savillex vials  
141 on a hotplate for ~2 days. Following digestion, the samples were dried in concentrated HNO<sub>3</sub> several  
142 times, and then converted to Cl<sup>-</sup> form by repeatedly drying the samples in 6 M HCl–0.06 M HF at  
143 ~120 °C. Finally, the samples were re-dissolved completely in 40 ml 6 M HCl–0.06 M HF. From  
144 these solutions ~5-10 % aliquots were spiked with a <sup>183</sup>W tracer that was previously calibrated against  
145 a pure W metal (Kleine et al., 2004) for the determination of W concentrations by isotope dilution.

146 For the isotope composition measurements, W was separated from the sample matrix using a  
147 two-stage anion exchange chromatography (Kruijer et al., 2015, 2014). The first column consists of a  
148 polyethylene transfer pipette (30 cm × 4 mm ø) filled with 4 ml of anion exchange resin (Biorad®  
149 AG1×8, 200-400 mesh), and serves to separate W from most matrix elements. Since the  
150 chromatographic separation is optimized for samples weighing <0.5 g, the individual digestions of the  
151 OJP samples (i.e. ~1.1 to ~2.1 g) were split in corresponding fractions of ~0.5 g equivalent sample  
152 weight. Thus, prior to the chromatography, each OJP sample was dried, and then re-dissolved in  
153 appropriate volumes of loading solution. Each sample fraction corresponding to ~0.5 g sample weight  
154 was loaded onto the column in 75 ml 0.5 M HCl–0.5 M HF. Following a rinse using 10 ml 0.5 M  
155 HCl–0.5 M HF, W was eluted in 15 ml 6 M HCl–1 M HF. After evaporating the sample solutions to  
156 dryness, a few drops of concentrated HClO<sub>4</sub> were added and then evaporated at 190-200 °C on a  
157 hotplate. This step was repeated once or twice. Subsequently, several drops of concentrated HF were  
158 added and evaporated at 200 °C several times until all HClO<sub>4</sub> was removed. Using such high  
159 temperature dry-downs in HClO<sub>4</sub> has several important advantages. First, HClO<sub>4</sub> efficiently destroys  
160 any organic molecules added to the sample during column chromatography. Second, as Os is highly  
161 volatile, drying samples in HClO<sub>4</sub> at high temperature ensures that any Os potentially remaining after  
162 the chemistry is effectively removed, resulting in sample solutions having <sup>188</sup>Os/<sup>183</sup>W of <0.00001.

163 Such small Os amounts cause any isobaric interferences from Os on W isotopes to be minimal  
164 (Section 2.2). Third, using HClO<sub>4</sub> results in significantly higher total W yields after chemical  
165 separation. This is because W tends to adhere to Teflon, resulting in loss of W in Savillex beakers.  
166 Finally, and related to the previous point, addition of HClO<sub>4</sub> appears to reduce the magnitude of any  
167 analytical <sup>183</sup>W effect (Section 4).

168 Following the HClO<sub>4</sub> and HF dry-downs, the samples were re-dissolved in 3.6 ml of 1 M HF.  
169 The purpose of the second column is to separate W from most other high field strength elements  
170 (HFSE; Nb, Hf, Ti, Zr). Approximately ~20 min. prior to loading, 0.080 ml H<sub>2</sub>O<sub>2</sub> (30% w/w) and 2.32  
171 ml H<sub>2</sub>O were added to the 3.6 ml 1 M HF sample solutions, and then placed on a hotplate (~100 °C)  
172 for ~15 min. Commercial 10 ml Biorad<sup>®</sup> Polyprep columns were filled with 1 ml anion exchange  
173 resin (BioRad<sup>®</sup> AG1×8, 200-400 mesh). After cleaning and conditioning of the resin, the sample  
174 solutions are loaded in 6 ml 0.6 M HF–0.4% H<sub>2</sub>O<sub>2</sub>. This is followed by a rinse with 10 ml 1 M HCl–  
175 2% H<sub>2</sub>O<sub>2</sub> in which most of the Ti, Zr, and Nb are eluted. Following elution of the remaining Ti, Zr,  
176 and Ag with 9 ml 8 M HCl–0.01 M HF, W was collected using 8.5 ml 6 M HCl–1 M HF. After  
177 evaporating the W cuts to dryness, several drops of concentrated HClO<sub>4</sub> (180-200 °C) were added and  
178 evaporated. Following the dry downs in HClO<sub>4</sub> the W cuts were converted to F<sup>-</sup> form by evaporating  
179 the samples to dryness in concentrated HF several times, and subsequently re-dissolved in a 0.56 M  
180 HNO<sub>3</sub>–0.24 M HF running solutions. The total yields of the chemical separation for W were ~70-  
181 95%. Total procedural blanks were ~50-100 pg W for the isotope composition analyses and ~1-7 pg  
182 for the isotope dilution analyses, in both cases insignificant given the amounts analyzed (~25-30 ng  
183 W).

184

## 185 2.2. Mass spectrometry

186 The W isotope measurements were performed using a ThermoScientific<sup>®</sup> Neptune *Plus* MC-  
187 ICPMS at the Institut für Planetologie in Münster. Samples and standards for W isotope analyses were  
188 introduced using self-aspirating C-flow PFA nebulizers (~50 µl/min) connected to a Cetac<sup>®</sup> Aridus II  
189 desolvator. The W isotope measurements were performed in low-resolution mode using high-  
190 sensitivity ‘Jet’ sample and ‘X’-skimmer cones, which yielded total ion beams of ~1.5-2.5 ×10<sup>-10</sup> A  
191 for a ~30 ppb W standard solution at an uptake rate of ~50 µl/min. All four major W isotopes (<sup>182</sup>W,  
192 <sup>183</sup>W, <sup>184</sup>W, <sup>186</sup>W) were measured simultaneously. Electronic baselines (60 s) were obtained prior to  
193 each sample measurement by deflecting the beam using the electrostatic analyzer and then subtracted  
194 from sample signal intensities. A single W isotope measurement comprised 200 cycles of 4.2 s  
195 integration time each. Note that, following the chemical separation, the different W cuts of the two  
196 OJP samples derived from individual columns were recombined so that ~25-30 ng of W was available  
197 for each individual sample measurement. Using this approach, the total available amount of W  
198 separated from the OJP samples was sufficient for five isotope ratio measurements of 200 cycles  
199 (Table 1). The reference materials analyzed here (BHVO-2, BCR-2) have higher W concentrations,  
200 and so each processed standard (~0.5 g) was analyzed several times (*i.e.*, 2-4 times 200 cycles). Small  
201 isobaric interferences from <sup>184</sup>Os and <sup>186</sup>Os on W isotope ratios were corrected by monitoring  
202 interference-free <sup>188</sup>Os, and were smaller than 10 parts-per-million (ppm) on <sup>182</sup>W/<sup>184</sup>W and hence  
203 insignificant. Instrumental mass bias was corrected by internal normalization to <sup>186</sup>W/<sup>184</sup>W = 0.92767  
204 (denoted ‘6/4’) or <sup>186</sup>W/<sup>183</sup>W = 1.9859 (denoted ‘6/3’) using the exponential law. The W isotope  
205 analyses of samples were bracketed by measurements of terrestrial solution standards (Alfa Aesar<sup>®</sup>,  
206 batch no. 22312) and results are reported as µ-unit deviations from the mean W isotope ratios of the  
207 bracketing solution standards, whose concentrations matched those of the sample solutions to within  
208 ~10%. Note that analyses of a different commercially available solution standard (NIST SRM 3163)

209 which has been used in several other W isotope studies by MC-ICPMS (*e.g.*, Willbold et al., 2011,  
210 2015; Krabbe et al., 2017) yield W isotope compositions identical to the Alfa Aesar bracketing  
211 standard solution (see Kruijer et al., 2012).

### 212 3. Results

213 The terrestrial reference materials (BHVO-2, BCR-2) analyzed here exhibit  $\mu^{182}\text{W}$  (6/4) values  
214 that are indistinguishable from the bracketing solution standard analyses (Table S1; Fig. 1-3), with a  
215 mean  $\mu^{182}\text{W}$  (6/4) of  $-1.9 \pm 11.0$  (2s.d.,  $N=132$ ). However, the same reference materials also exhibit  
216 small and variable W isotope anomalies for normalizations involving  $^{183}\text{W}$  (Fig. 2, 3), with coupled  
217 excesses in  $\mu^{182}\text{W}$  (6/3) [up to +30 ppm] and  $\mu^{184}\text{W}$  (6/3) [up to +15 ppm], and corresponding deficits  
218 in  $\mu^{183}\text{W}$  (6/4) [down to -23 ppm] (Fig. 2c, 2d). Of note, similar W isotope systematics are observed  
219 for the OJP samples analyzed in this study. Again, the OJP samples analyzed here exhibit  $\mu^{182}\text{W}$  (6/4)  
220 values that are indistinguishable from the bracketing standard solution analyses (Table 1; Fig. 2, 4),  
221 where the mean  $\mu^{182}\text{W}$  (6/4) of five replicate measurements corresponds to  $-0.4 \pm 5.1$  (95% conf.,  $N=5$ ;  
222 Table 1). Nevertheless, similar to the reference materials, the same OJP samples also exhibit small  
223 and variable W isotope anomalies for normalizations involving  $^{183}\text{W}$  (Table 1; Fig. 2, 4), with coupled  
224 excesses in  $\mu^{182}\text{W}$  (6/3) [up to +33 ppm] and  $\mu^{184}\text{W}$  (6/3) [up to +17 ppm], and corresponding  
225 deficits in  $\mu^{183}\text{W}$  (6/4) [down to -25 ppm] (Fig. 2c, 2d). Finally, the five OJP samples analyzed here  
226 display very similar and relatively low W concentrations of between ~13 and ~17 ppb.

### 227 4. Accuracy and reproducibility of W isotope measurements by MC-ICPMS

228 The accuracy and reproducibility of the W isotope measurements by MC-ICPMS were assessed  
229 through analyses of terrestrial reference materials (BHVO-2, BCR-2) that were digested, processed  
230 and analyzed alongside the OJP samples. Although these two reference materials have higher W  
231 contents than the OJP samples analyzed, they were nevertheless selected because a large body of  
232 high-precision W isotopic data from different laboratories (Bristol, Maryland, Münster) and acquired  
233 using different measurement techniques (MC-ICPMS, NTIMS) exists for these reference materials.  
234 Moreover, the analyses performed here are complemented by additional analyses of BHVO-2 and  
235 BCR-2 performed in the Münster lab since 2012, allowing assessment of the long-term reproducibility  
236 of the measurements from the present study. The mean  $\mu^{182}\text{W}$  (6/4) values for BHVO-2 and BCR-2  
237 obtained in the present study, and including data from the Münster laboratory since 2012, are  $-$   
238  $2.2 \pm 11.2$  (2s.d.,  $N=107$ ) and  $0.7 \pm 7.9$  ( $N=13$ ), respectively. Thus, for both samples,  $\mu^{182}\text{W}$  is  
239 statistically indistinguishable from the composition of the solution standard (Fig. 1a). The two-  
240 standard deviation (2s.d.) of  $\pm 11$  ppm obtained for the BHVO-2 measurements provides a  
241 conservative estimate of the external reproducibility of a *single* W isotope measurement (200 cycles).  
242 Of note, a similar reproducibility is obtained for analyses of a terrestrial metal standard NIST129c  
243 (Mean  $\mu^{182}\text{W} = +1.3 \pm 9.3$ , 2s.d.,  $N=53$ ) (Fig. 1b), and our method for high-precision W isotope  
244 analyses can therefore also be used to analyze metal samples including iron meteorites (see *e.g.*,  
245 Kruijer et al., 2014). Altogether, the technique thus yields accurate and precise  $\mu^{182}\text{W}$  (6/4) values for  
246 a measurement consuming as little as 30 ng of W. Provided sufficient W is available, the precision for  
247 a single W isotope measurement as quoted above can be further improved by pooling several  
248 individual W isotope measurements (*i.e.*, solution replicates) of any given sample. Such a pooled W  
249 isotope measurement typically consumes ~150 ng W (*i.e.*,  $5 \times 30$  ng) and yields an uncertainty on  
250  $\mu^{182}\text{W}$  (6/4) of *ca.* 5 ppm (95% conf., with  $N=5$ ), where the 95% conf. limits are calculated according  
251 to  $(\text{s.d.} \times t_{0.95, N-1}) / \sqrt{N}$ . For the processed reference materials, the mean  $\mu^{182}\text{W}$  (6/4) of BHVO-2 and  
252 NIST129c calculated in this manner correspond to  $-2.3 \pm 5.6$  ppm (95% conf.,  $N=20$ ) and  $1.0 \pm 5.5$  ppm

253 ( $N=12$ ), demonstrating that W isotope compositions of natural samples can be accurately be  
254 determined to high precision.

255 In contrast to the  $\mu^{182}\text{W}$  (6/4) values discussed above, the W isotope normalizations involving  
256  $^{183}\text{W}$  exhibit considerably more scatter. In particular, geological reference materials (BHVO-2, BCR-  
257 2) as well as the metal standard (NIST129c) exhibit small, but in some cases resolvable deficits in  
258  $\mu^{183}\text{W}$  (6/4) that are coupled with small excesses in  $\mu^{182}\text{W}$  (6/3) and  $\mu^{184}\text{W}$  (6/3) (Fig. 2a, 2b). These  
259 coupled W isotope variations have been observed in several prior high-precision W isotope studies  
260 (*e.g.*, Budde et al., 2016; Cook et al., 2014; Dale et al., 2017; Kruijer et al., 2012; Willbold et al.,  
261 2011) and are caused by an analytical mass-independent isotope fractionation resulting in apparent  
262 deficits in  $^{183}\text{W}$  (henceforth referred to as ‘analytical  $^{183}\text{W}$  effect’). Previous studies demonstrated that  
263 this analytical  $^{183}\text{W}$  effect is probably not caused by the column chromatography, but instead is most  
264 likely caused by incomplete re-dissolution of W following evaporation of solutions in Savillex vials  
265 (Kruijer et al., 2012; Willbold et al., 2011). Moreover, Cook and Schönbachler (2016) showed that the  
266 W isotope systematics related to the  $^{183}\text{W}$  effect are consistent with a nuclear field shift effect  
267 resulting in a mass-independent isotope fractionation affecting primarily the odd W isotopes (*i.e.*,  
268  $^{183}\text{W}$ ). For each individual sample, the  $\mu^{182}\text{W}$  (6/3) values can therefore be corrected using its  
269 measured  $\mu^{184}\text{W}$  (6/3) and the following relation (Kruijer et al., 2012; Cook and Schönbachler,  
270 2016):  $\mu^{182}\text{W}$  (6/3)<sub>corrected</sub> =  $\mu^{182}\text{W}$  (6/3)<sub>measured</sub> - 1.962 ×  $\mu^{184}\text{W}$  (6/3). Even though the nuclear field  
271 shift theoretically also slightly modifies  $\mu^{182}\text{W}$  (6/4) values, the magnitude of this effect is ~16 times  
272 smaller than the effect on  $\mu^{184}\text{W}$  (6/3), and hence, essentially negligible. Nevertheless, to be fully  
273 consistent, the above approach was used here to correct both the  $\mu^{182}\text{W}$  (6/4) and  $\mu^{182}\text{W}$  (6/3) of  
274 individual BHVO-2 and BCR-2 standards. After the correction, the mean  $\mu^{182}\text{W}$  (6/4) and  $\mu^{182}\text{W}$   
275 (6/3) for BHVO-2 and BCR-2 are indistinguishable to within <0.1 ppm (Table S1), demonstrating  
276 that the nuclear field shift effect very accurately describes the observed difference between  $\mu^{182}\text{W}$   
277 (6/4) and  $\mu^{182}\text{W}$  (6/3) for processed standards and samples.

278 The analytical  $^{183}\text{W}$  effect presents somewhat of a challenge when precise analyses of non-  
279 radiogenic W isotopes are required (*i.e.*,  $\mu^{183}\text{W}$  and  $\mu^{184}\text{W}$ ), as in studies focused on identifying  
280 nucleosynthetic W isotope heterogeneities in meteorites and their components (*e.g.*, Burkhardt et al.,  
281 2012; Kruijer et al., 2014). Accordingly, in such studies the magnitude of any analytical  $^{183}\text{W}$  effect  
282 must be closely monitored by analyzing a wide range of terrestrial reference materials. Nevertheless,  
283 for studies where only precise  $\mu^{182}\text{W}$  data are required, the analytical  $^{183}\text{W}$  effect does not present an  
284 issue. This is because the  $^{183}\text{W}$  effect affect modifies  $\mu^{182}\text{W}$  (6/4) values only to a very minor degree,  
285 and consequently most recent MC-ICPMS studies investigating  $\mu^{182}\text{W}$  variations in terrestrial and  
286 (some) extraterrestrial samples have exclusively used the  $\mu^{182}\text{W}$  (6/4) normalization (Dale et al.,  
287 2017; Kruijer et al., 2017, 2015). Thus, the  $^{183}\text{W}$  effect is irrelevant when precisely determining  $\mu^{182}\text{W}$   
288 (6/4) variations by MC-ICPMS in terrestrial rocks, including the OJP samples analyzed here.  
289 Nevertheless, some previous NTIMS studies, including the OJP study of Rizo et al. (2016), relied on a  
290 double normalization procedure employing  $\mu^{183}\text{W}$ , and consequently, as discussed below, the  $^{183}\text{W}$   
291 effect may pose an issue for obtaining accurate  $\mu^{182}\text{W}$  data using this technique.

## 292 **5. Agreement between recent high-precision W isotope studies**

293 The potential presence of an analytical  $^{183}\text{W}$  effect raises the question of how good the agreement  
294 is between different recent high-precision W isotope studies. Tungsten isotope analyses of the same  
295 samples but conducted by different laboratories generally reproduce very well (Fig. 5). For example,  
296 for a pillow basalt sample from Isua, Greenland (SM/GR/00/26), two MC-ICPMS studies, conducted  
297 in different labs, obtained indistinguishable  $\mu^{182}\text{W}$  excesses of *ca.* +11 to +13 ppm (Dale et al., 2017;

298 Willbold et al., 2011). Similarly, for two KREEP-rich lunar samples (68115, 68815), two recent  
299 studies reported indistinguishable  $\mu^{182}\text{W}$  excesses of *ca.* +25 ppm (Kruijer et al., 2015; Touboul et al.,  
300 2015). Similar good agreement is seen for analyses of meteorites. For instance, for the IVB iron  
301 meteorite Skookum, indistinguishable  $\mu^{182}\text{W}$  values of  $-330\pm 4$  and  $-335\pm 6$  were obtained by MC-  
302 ICPMS and NTIMS (Kruijer et al., 2013, 2014; Archer et al., 2017). Collectively, these examples  
303 demonstrate that reproducible and precise  $\mu^{182}\text{W}$  data can be obtained using both MC-ICPMS and N-  
304 TIMS techniques.

305 However, in detail some disparities between laboratories become apparent for materials that have  
306 been analyzed very often, such as geological reference material BHVO-2 (Fig. 5). Whereas the mean  
307  $\mu^{182}\text{W}$  values for BHVO-2 obtained here and by Willbold et al. (2011, 2015) are essentially  
308 indistinguishable from other standards, geological reference materials and most modern terrestrial  
309 rocks, Mundl et al. (2017) and Mei et al. (2018) reported small but resolved deficits for BHVO-2  
310 down to *ca.* -9 ppm. The exact cause of these apparent small-scale  $^{182}\text{W}$  variations for BHVO-2  
311 remains unclear, and resolving this issue will require future W isotope analyses of the same BHVO-2  
312 powder digestion by different laboratories. Overall the BHVO-2 data highlight that determining  
313  $\mu^{182}\text{W}$  variations of  $< \sim 10$  ppm is analytically extremely challenging. In particular, as will be  
314 illustrated below, at this level precision other analytical effects, including the nuclear field shift effect  
315 described above, potentially become problematic.

## 316 **6. No $^{182}\text{W}$ anomaly in the Ontong Java Plateau Source**

317 Despite the overall good agreement between several W isotope studies, W isotope measurements  
318 of drill core samples from the Ontong Java Plateau do exhibit inconsistencies. In particular, the mean  
319  $\mu^{182}\text{W}$  (6/4) obtained for the OJP samples analyzed here corresponds to  $-0.4\pm 5.1$  ppm (95% conf.,  
320  $N=5$ ). This value is indistinguishable from the value of the present-day bulk silicate Earth as defined  
321 by the bracketing solution standard as well as the processed terrestrial reference materials analyzed in  
322 this study. Moreover, the same OJP samples exhibit coupled variations in  $\mu^{182}\text{W}$  (6/3),  $\mu^{184}\text{W}$  (6/3),  
323 and  $\mu^{183}\text{W}$  (6/4) which closely mirror those observed for the terrestrial reference materials in this  
324 study (Fig. 2,4). These variations, therefore, must be analytical in origin, and are very likely caused by  
325 a nuclear field shift effect induced during sample preparation (Section 4). Consequently, our results  
326 do not provide evidence for a resolved  $\mu^{182}\text{W}$  anomaly in rocks from the Ontong Java Plateau. This is  
327 consistent with the findings of Willbold et al. (2011), who analyzed a OJP sample from the same drill  
328 core (*i.e.*, 192-1187A-006R-06W) and also did not find a resolved  $^{182}\text{W}$  anomaly. Furthermore,  
329 Willbold et al. (2011) also reported ‘normal’  $\mu^{182}\text{W}$  compositions for a sample from another OJP core  
330 (192-1185A), as well as for several samples from two other large igneous provinces in the western  
331 Pacific Ocean, including the related Manihiki-Plateau and the Shatsky Rise.

332 Contrary to the results from this and the Willbold et al. (2011) study, Rizo et al (2016a) reported  
333 a well-resolved  $\mu^{182}\text{W}$  excess of *ca.* +24 ppm in an OJP sample (192-1187A-009R-04W). One  
334 potential explanation for the discrepancy between the studies is that there are true  $\mu^{182}\text{W}$   
335 heterogeneities within the Ontong Java Plateau. However, not only are the samples from this study  
336 and that of Rizo et al. (2016a) from the same drill core, they also derive from the same lava flow and  
337 were sampled in very close proximity to each other (as little as  $\sim 6$  cm apart; see Fig. S1). Moreover,  
338 all samples from this part of the core belong to the same lithologic unit (Kroenke type; Fitton and  
339 Godard, 2004) and as such exhibit strong geochemical similarities. Consequently, it seems extremely  
340 unlikely that  $\mu^{182}\text{W}$  heterogeneities exist among the OJP samples analyzed here and by Rizo et al.  
341 (2016a). Another explanation for the disparity between the studies could be that the source  $\mu^{182}\text{W}$   
342 signatures of the OJP samples are variably affected by contamination with W from a ‘normal’  $\mu^{182}\text{W}$

343 source (*i.e.*,  $\mu^{182}\text{W} = 0$ ). However, both OJP samples analyzed here (Table 1) and those by Rizo et al.  
344 (2016a) exhibit very similar and low W concentrations between ~13 and ~23 ppb, where the samples  
345 from the present study have W concentrations at the lower end of this range. Thus, W contamination  
346 from another source (*e.g.* from the drill core, crustal rocks, or seawater) can effectively be ruled as the  
347 cause of the disparity in  $\mu^{182}\text{W}$  between the studies.

348 This leaves an unaccounted analytical  $^{183}\text{W}$  effect as the most likely cause for the disparate  $^{182}\text{W}$   
349 results for OJP samples reported in this and the Rizo et al. (2016a) study. The  $\mu^{183}\text{W}$  analyses of the  
350 terrestrial reference materials and OJP samples in the present study (Table 1) demonstrate that  
351 analytical  $\mu^{183}\text{W}$  deficits of up to several tens of ppm are not atypical. This is especially true for large  
352 samples with relatively low yields such as the OJP samples analyzed by Rizo et al. (2016a) (see also  
353 below). Such analytical  $\mu^{183}\text{W}$  deficits are problematic in case of W isotope measurements by NTIMS  
354 because such analyses require a double normalization to correct for instrumental mass fractionation  
355 and therefore have to utilize W isotope ratios involving  $^{183}\text{W}$ . More specifically, for W isotope  
356 compositions determined by N-TIMS, the measured (and mass fractionation corrected)  $^{182}\text{W}/^{184}\text{W}$  and  
357  $^{183}\text{W}/^{184}\text{W}$  of standards exhibit a residual positive correlation (Touboul and Walker, 2011). These  
358 correlated W isotope ratios have been attributed to a changing mass-dependent isotope fractionation  
359 of O isotopes in the TIMS source that causes variations in measured W-oxide isotope compositions,  
360 ultimately leading to residual variations in measured  $\mu^{182}\text{W}$  compositions on the order of ~100-150  
361 ppm (Touboul and Walker, 2011). Because the slope of the correlation line is invariant over time, the  
362 measured  $\mu^{182}\text{W}$  of a sample is typically corrected for this second order mass fractionation effect  
363 using the (constant) slope of the correlation line together with the measured  $^{183}\text{W}/^{184}\text{W}$  ratio of the  
364 sample (Fig. 6). This approach results in final  $\mu^{182}\text{W}$  values with a precision of  $\pm 5$  ppm (2s.d.) as long  
365 as the corresponding  $\mu^{183}\text{W}$  values are accurately and precisely determined (Touboul and Walker,  
366 2012). However, because measured  $\mu^{183}\text{W}$  values are needed to correct the  $\mu^{182}\text{W}$  values for this  
367 second-order mass fractionation, the N-TIMS method used by Rizo et al. (2016a) does not yield an  
368 independent measurement of  $\mu^{183}\text{W}$ . Thus, any mass-independent analytical effect on  $\mu^{183}\text{W}$  would go  
369 unnoticed in the NTIMS analyses. It therefore seems possible that the +24 ppm  $\mu^{182}\text{W}$  anomaly  
370 inferred for the OJP sample analyzed by Rizo et al. (2016) is caused by such an effect. For instance,  
371 an apparent +24 ppm  $\mu^{182}\text{W}$  anomaly would be inferred if the same sample had an analytical  $\mu^{183}\text{W}$   
372 deficit of similar magnitude, *i.e.*, -24 ppm (Fig. 6). It is important to note that this magnitude for the  
373  $^{183}\text{W}$  effect is well within the range of observed effects, including some of the OJP samples analyzed  
374 in the present study (Table 1). Accordingly, the +24 ppm  $\mu^{182}\text{W}$  anomaly reported by Rizo et al.  
375 (2016a) may be caused by an analytical effect on  $^{183}\text{W}$ .

376 Although Rizo et al. (2016a) found resolved  $\mu^{182}\text{W}$  excesses for two samples (OJP sample 192-  
377 1187A-009R-04W and one Baffin Bay sample), they did not find such anomalies for the other  
378 samples they investigated. This raises the question as to why this might be the case, particularly given  
379 that the latter samples would likely also have been subjected to the analytical  $^{183}\text{W}$  effect. The answer  
380 may lie in the relatively low W concentrations of both the OJP and Baffin Bay samples (<23 ppb W)  
381 in comparison to the other samples as well as the terrestrial standards. As a consequence, whereas for  
382 most samples 'only' several grams of sample material had to be processed in order to have sufficient  
383 W for a single NTIMS analysis (~500 ng W), significantly larger sample amounts were required for  
384 the OJP sample and the Baffin Bay sample Pd-2 (~34 g and ~44 g, respectively). For this reason, the  
385 chemical separation for these two samples required the use of a large number of chromatography  
386 columns, and accordingly, the evaporation of large volumes of sample solution in Savillex vials on a  
387 hotplate. Given that the analytical  $^{183}\text{W}$  effect is very likely generated during incomplete re-  
388 dissolution of W in Savillex vials (Section 4), this extensive W separation procedure for the OJP and  
389 Baffin Bay samples might have magnified any analytical  $^{183}\text{W}$  effect in comparison to samples with

390 higher W amounts. Note that the relatively low procedural W yields for these two samples (~50%)  
391 would be consistent with this interpretation.

392 In summary, we have not reproduced the +24 ppm  $\mu^{182}\text{W}$  excess reported by Rizo et al. (2016a)  
393 for OJP samples, and the data presented here demonstrate that there is no  $^{182}\text{W}$  excess in rocks from  
394 the Ontong Java Plateau. As such, the results from this study also cast some doubt on the validity of  
395 the +48 ppm  $\mu^{182}\text{W}$  excess reported for a sample from Baffin Bay (Pd-2) as determined by NTIMS in  
396 the same analytical campaign (Rizo et al., 2016a). Reassessing the  $\mu^{182}\text{W}$  composition for samples  
397 from Baffin Bay will therefore be an important future task, ideally utilizing both MC-ICPMS and  
398 NTIMS studies. Finally, we note that Archer et al. (2017) recently developed a new N-TIMS  
399 technique for high-precision W isotope analysis that permits the independent and simultaneous  
400 measurement of  $^{18}\text{O}/^{16}\text{O}$  on  $\text{WO}_3^-$ . As a consequence, this new TIMS technique no longer relies on  
401 accurate  $\mu^{183}\text{W}$  analyses for obtaining precise  $\mu^{182}\text{W}$  measurements. Using this technique, it should in  
402 principle be possible to assess the occurrence of the analytical  $^{183}\text{W}$  effect in NTIMS analyses and to  
403 evaluate as to whether it has the same magnitude as in MC-ICPMS studies.

## 404 7. Conclusions

405 The results presented here and elsewhere demonstrate that an analytical  $^{183}\text{W}$  effect can  
406 potentially occur in any high-precision W isotope study. Thus, to avoid erroneous data and resulting  
407 misinterpretation, any high-precision W isotope study conducted by MC-ICPMS or NTIMS should  
408 assess whether such potential analytical  $^{183}\text{W}$  effects are significant. Such an assessment requires (i) a  
409 measurement technique permitting an independent measurement of  $\mu^{183}\text{W}$ , and (ii) the analysis of a  
410 sufficient number of terrestrial reference materials alongside the samples. Nevertheless, once the  $^{183}\text{W}$   
411 effect is taken into account, both MC-ICPMS and NTIMS can provide W isotope data that is accurate  
412 to within a very high level of precision (*i.e.*, down to *ca.* 5 ppm, 95% conf.).

413 The new data for OJP samples presented here demonstrate that there is no resolvable  $^{182}\text{W}$  excess  
414 in the Ontong Java Plateau source. This is consistent with results from a prior MC-ICPMS study  
415 (Willbold et al., 2011), but is in disagreement with the +24 ppm  $^{182}\text{W}$  excess reported for OJP samples  
416 in an NTIMS study (Rizo et al., 2016a). As such, these results also cast some doubt on the validity of  
417 the  $^{182}\text{W}$  excess reported for a single Baffin Bay sample in the same study that reported a resolved  
418  $^{182}\text{W}$  excess for the OJP samples (Rizo et al., 2016a). Assessing the  $^{182}\text{W}$  composition of Baffin Bay  
419 samples, therefore, will necessitate new high-precision W isotope measurements, ideally using both  
420 MC-ICPMS and NTIMS.

421 One important implication of the present study is that  $\mu^{182}\text{W}$  excesses in terrestrial rocks seem to  
422 be restricted to a narrow range between *ca.* +10 and +15 ppm relative to the modern bulk silicate  
423 Earth. Excesses of this magnitude can readily be accounted for by late accretion, implying that these  
424  $^{182}\text{W}$  excesses do not require the preservation of early mantle heterogeneities that have been generated  
425 prior to the Moon-forming impact.

426  
427 **Acknowledgements:** We thank the Ocean Drilling Program (ODP) for providing the drill core  
428 samples from the Onton Java Plateau for this study. We further thank Mike Coffin for this help with  
429 selecting samples. We also thank the editor, K. Mezger, and the reviewers T. Elliott and M. Willbold  
430 for constructive comments that helped improve the paper. This work was funded by the Deutsche  
431 Forschungsgemeinschaft (SFB TRR 170 subproject C3-1). This is TRR 170 publication no. XX.

432  
433

- 435 Archer, G.J., Mundl, A., Walker, R.J., Worsham, E.A., Bermingham, K.R., 2017. High-precision  
436 analysis of  $^{182}\text{W}/^{184}\text{W}$  and  $^{183}\text{W}/^{184}\text{W}$  by negative thermal ionization mass spectrometry: Per-  
437 integration oxide corrections using measured  $^{18}\text{O}/^{16}\text{O}$ . *Int. J. Mass Spectrom.* 414, 80–86.
- 438 Budde, G., Kleine, T., Kruijjer, T.S., Burkhardt, C., Metzler, K., 2016. Tungsten isotopic constraints  
439 on the age and origin of chondrules. *Proc. Natl. Acad. Sci. U. S. A.* 113, 2886–2891.  
440 doi:10.1073/pnas.1524980113
- 441 Cook, D.L., Kruijjer, T.S., Leya, I., Kleine, T., 2014. Cosmogenic  $^{180}\text{W}$  variations in meteorites and  
442 re-assessment of a possible  $^{184}\text{Os}$ – $^{180}\text{W}$  decay system. *Geochim. Cosmochim. Acta* 140, 160–  
443 176. doi:10.1016/j.gca.2014.05.013
- 444 Cook, D.L., Schönbächler, M., 2016. High-precision measurement of W isotopes in Fe–Ni alloy and  
445 the effects from the nuclear field shift. *J. Anal. At. Spectrom.* 31, 1400–1405.  
446 doi:10.1039/C6JA00015K
- 447 Dale, C.W., Kruijjer, T.S., Burton, K.W., 2017. Highly siderophile element and  $^{182}\text{W}$  evidence for a  
448 partial late veneer in the source of 3.8 Ga rocks from Isua, Greenland. *Earth Planet. Sci. Lett.*  
449 458, 394–404.
- 450 Day, J.M.D., 2016. Evidence against an ancient non-chondritic mantle source for North Atlantic  
451 Igneous Province lavas. *Chemical Geology* 440, 91–100.
- 452 Fitton, G.F., Godard, M., 2004. Origin and evolution of magmas on the Ontong Java Plateau. *Geol.*  
453 *Soc. London, Spec. Publ.* 229, 151–178.
- 454 Foley, C.N., Wadhwa, M., Borg, L.E., Janney, P.E., Hines, R., Grove, T.L., 2005. The early  
455 differentiation history of Mars from  $^{182}\text{W}$ – $^{142}\text{Nd}$  isotope systematics in the SNC meteorites.  
456 *Geochim. Cosmochim. Acta* 69, 4557–4571. doi:10.1016/j.gca.2005.05.009
- 457 Harper, C.L., Volkening, J., Heumann, K.G., Shih, C.Y., Wiesmann, H., 1991.  $^{182}\text{Hf}$ – $^{182}\text{W}$ : new  
458 cosmochronometric constraints on terrestrial accretion, core formation, the astrophysical site of  
459 the r-process, and the origin of the Solar System, in: *Lunar Planet. Sci. Conf. Abstr.* p. 22: 515–  
460 516.
- 461 Jacobsen, S. B. (2005) The Hf–W isotopic system and the origin of the Earth and Moon. *Ann. Rev.*  
462 *Earth Planet. Sci.* 33, 531– 570.
- 463 Jackson, M.G., Carlson, R.W., Kurz, M.D., Kempton, P.D., Francis, D., Blusztajn, J., 2011. Evidence  
464 for the survival of the oldest terrestrial mantle reservoir. *Nature* 466, 853–856.
- 465 Kleine, T., Mezger, K., Münker, C., Palme, H., Bischoff, A., 2004.  $^{182}\text{Hf}$ – $^{182}\text{W}$  isotope systematics of  
466 chondrites, eucrites, and martian meteorites: Chronology of core formation and early mantle  
467 differentiation in Vesta and Mars. *Geochim. Cosmochim. Acta* 68, 2935–2946.  
468 doi:10.1016/j.gca.2004.01.009
- 469 Kleine, T., Münker, C., Mezger, K., Palme, H., 2002. Rapid accretion and early core formation on  
470 asteroids and the terrestrial planets from Hf–W chronometry. *Nature* 418, 952–5.  
471 doi:10.1038/nature00982
- 472 Kleine, T., Walker, R.J. (2017) Tungsten isotopes in planets. *Annu. Rev. Earth Planet. Sci.* 2017. 45,  
473 389–417.
- 474 Krabbe N., Kruijjer T.S., Kleine T. (2017) Tungsten stable isotope compositions of terrestrial samples  
475 and meteorites determined by double spike MC-ICPMS. *Chemical Geology* 450, 135–154.
- 476 Kruijjer, T.S., Fischer-Gödde, M., Kleine, T., Sprung, P., Leya, I., Wieler, R. (2013) Neutron capture  
477 on Pt isotopes in iron meteorites and the Hf–W chronology of core formation in planetesimals.  
478 *Earth Planet. Sci. Lett.* 361, 162–172.

- 479 Kruijjer, T.S., Kleine, T., Fischer-Gödde, M., Burkhardt, C., Wieler, R., 2014. Nucleosynthetic W  
480 isotope anomalies and the Hf-W chronometry of Ca-Al-rich inclusions. *Earth Planet. Sci. Lett.*  
481 403, 317–327. doi:10.1016/j.epsl.2014.07.003
- 482 Kruijjer, T.S., Touboul, M., Fischer-Gödde, M., Bermingham, K.R., Walker, R.J., Kleine, T., 2014b.  
483 Protracted core formation and rapid accretion of protoplanets. *Science* 344, 1150–1154.  
484 <http://dx.doi.org/10.1126/science.1251766>.
- 485 Kruijjer, T.S., Kleine, T., Fischer-Gödde, M., Sprung, P., 2015. Lunar tungsten isotopic evidence for  
486 the late veneer. *Nature* 520, 534–537. doi:10.1038/nature14360
- 487 Kruijjer, T.S., Sprung, P., Kleine, T., Leya, I., Burkhardt, C., Wieler, R., 2012. Hf–W chronometry of  
488 core formation in planetesimals inferred from weakly irradiated iron meteorites. *Geochim.*  
489 *Cosmochim. Acta* 99, 287–304. doi:10.1016/j.gca.2012.09.015
- 490 Kruijjer, T.S., Kleine, T., Borg, L.E., Brennecka, G.A., Irving, A.J., Agee, C.B., 2017. The early  
491 differentiation of Mars inferred from Hf–W chronometry. *Earth Planet. Sci. Lett.* 474, 345–354.
- 492 Liu, J., Touboul, M., Ishikawa, A., Walker, R.J., Pearson, D.G., 2016. Widespread tungsten isotope  
493 anomalies and W mobility in crustal and mantle rocks of the Eoarchean Saglek Block, northern  
494 Labrador, Canada: implications for early Earth processes and W recycling. *Earth Planet. Sci.*  
495 *Lett.* 448, 13–23.
- 496 Mei, Q-F., Yang, J-H., Yang, Y-H. (2018) An improved extraction chromatographic purification of  
497 tungsten from a silicate matrix for high precision isotopic measurements using MC-ICPMS. *J.*  
498 *Anal. At. Spectrom.*, doi:10.1039/C8JA00024G.
- 499 Mundl, A., Touboul, M., Jackson, M.G., Day, J.M.D., Kurz, M.D., Lekic, V., Helz, R.T., Walker,  
500 R.J., 2017. Tungsten-182 heterogeneity in modern ocean island basalts. *Science* 356, 66–69.
- 501 Neal, C.R., Mahoney, J.J., Kroenke, L.W., Duncan, R.A., Petterson, M.G., 1997. The Ontong Java  
502 Plateau. *Geophys. Monogr. Ser.* 100, 183–216.
- 503 Puchtel, I.S., Blichert-Toft, J., Touboul, M., Horan, M.F., Walker, R.J., 2016. The coupled  $^{182}\text{W}$ - $^{142}\text{Nd}$   
504 record of early terrestrial mantle differentiation. *Geochemistry, Geophys. Geosystems* 17, 2168–  
505 2193.
- 506 Righter, K., Shearer, C.K., 2003. Magmatic fractionation of Hf and W: constraints on the timing of  
507 core formation and differentiation in the Moon and Mars. *Geochim. Cosmochim. Acta* 67,  
508 2497–2507. doi:10.1016/S0016-7037(02)01349-2
- 509 Rizo, H., Walker, R.J., Carlson, R.W., Horan, M., Mukhopadhyay, S., Manthos, V., Francis, D.,  
510 Jackson, M.G., 2016a. Preservation of Earth-forming events in the tungsten isotopic  
511 composition of modern flood basalts. *Science* 352, 809–812.
- 512 Rizo, H., Walker, R.J., Carlson, R.W., Touboul, M., Horan, M.F., Puchtel, I.S., Boyet, M., Rosing,  
513 M.T., 2016b. Early Earth differentiation investigated through  $^{142}\text{Nd}$ ,  $^{182}\text{W}$ , and highly siderophile  
514 element abundances in samples from Isua, Greenland. *Geochim. Cosmochim. Acta* 175, 319–  
515 336.
- 516 Touboul, M., Liu, J., O’Neil, J., Puchtel, I.S., Walker, R.J., 2014. New insights into the Hadean  
517 mantle revealed by  $^{182}\text{W}$  and highly siderophile element abundances of supracrustal rocks from  
518 the Nuvvuagittuq Greenstone Belt, Quebec, Canada. *Chem. Geol.* 383, 63–75.  
519 doi:10.1016/j.chemgeo.2014.05.030
- 520 Touboul, M., Puchtel, I.S., Walker, R.J., 2015. Tungsten isotopic evidence for disproportional late  
521 accretion to the Earth and Moon. *Nature* 520, 530–533. doi:10.1038/nature14355
- 522 Touboul, M., Puchtel, I.S., Walker, R.J., 2012.  $^{182}\text{W}$  evidence for long-term preservation of early  
523 mantle differentiation products. *Science* 335, 1065–9. doi:10.1126/science.1216351
- 524 Touboul, M., Walker, R.J., 2011. High precision tungsten isotope measurement by thermal ionization

- 525 mass spectrometry. *Int. J. Mass Spectrom.* doi:10.1016/j.ijms.2011.08.033
- 526 Willbold, M., Elliott, T., Moorbath, S., 2011. The tungsten isotopic composition of the Earth's mantle  
527 before the terminal bombardment. *Nature* 477, 195–8. doi:10.1038/nature10399
- 528 Willbold, M., Mojzsis, S.J., Elliott, T., Chen, H.-W., 2015. Tungsten isotope composition of the  
529 Acasta Gneiss Complex. *Earth Planet. Sci. Lett.* 419, 168–177.
- 530 Yin, Q., Jacobsen, S.B., Yamashita, K., Blichert-Toft, J., Télouk, P., Albarède, F., 2002. A short  
531 timescale for terrestrial planet formation from Hf-W chronometry of meteorites. *Nature* 418,  
532 949–52. doi:10.1038/nature00995
- 533
- 534

535 **Figure captions**

536 **Fig. 1:**  $\mu^{182}\text{W}$  compositions of terrestrial reference materials. Each data point represents a single W  
537 isotope measurement of a reference material that was processed through the full chemical separation  
538 (a) Basalt standards (BHVO-2 and BCR-2), and (b) metal standard NIST 129c. Error bars denote two  
539 standard errors (2s.e.) obtained from internal run statistics. The external reproducibility (2 s.d.) of a  
540 single W isotope measurement (200 cycles) as inferred from replicate standard analyses is shown as a  
541 light gray filled bar, and the corresponding 95% confidence limits as a dark gray bar. Data sources:  
542 This study (open symbols), Budde et al. (2016, 2017) and Kruijjer et al. (2015, 2017a, 2017b, 2017c)  
543 (closed symbols).

544

545 **Fig. 2:**  $\mu^{182}\text{W}$  vs.  $\mu^{183}\text{W}$  (or  $\mu^{184}\text{W}$ ) data of reference materials and OJP samples analyzed in this  
546 study. Each data point represents a single W isotope analysis (200 cycles) and error bars represent two  
547 standard errors (2s.e.) obtained from internal run statistics. (a) Terrestrial reference materials (BHVO-  
548 2, BCR-2, NIST129c), and (b) OJP samples plotted together with reference material analyses.  
549 Distinguished are BHVO-2 data from this study (open symbols) and from prior studies (closed  
550 symbols) conducted by the Münster group. Solid lines depict trajectories predicted for analytical  $^{183}\text{W}$   
551 deficits (Kruijjer et al., 2012; Cook and Schönbächler, 2016). Data sources: This study (open  
552 symbols), Budde et al. (2016, 2017) and Kruijjer et al. (2015, 2017a, 2017b, 2017c).

553

554 **Fig. 3:** Quintuple  $\mu^{182}\text{W}$  measurements of terrestrial reference materials BHVO-2, BCR-2, and  
555 NIST129c. Each data point represents the mean of five W isotope measurements (200 cycles) and  
556 error bars denote 95% conf. limits. Shaded area shows the mean of all quintuple measurements  
557 ( $N=35$ ) and the associated reproducibility (2s.d).

558

559 **Fig. 4:**  $\mu^{182}\text{W}$  vs.  $\mu^{183}\text{W}$  (or  $\mu^{184}\text{W}$ ) data of OJP samples analyzed in this work. The  $\mu^{182}\text{W}$  value  
560 reported by Rizo et al. (2016) is plotted for comparison (green shaded area). Each data point  
561 represents a single analysis of an OJP sample and error bars represent two standard errors (2s.e.)  
562 obtained from internal run statistics.

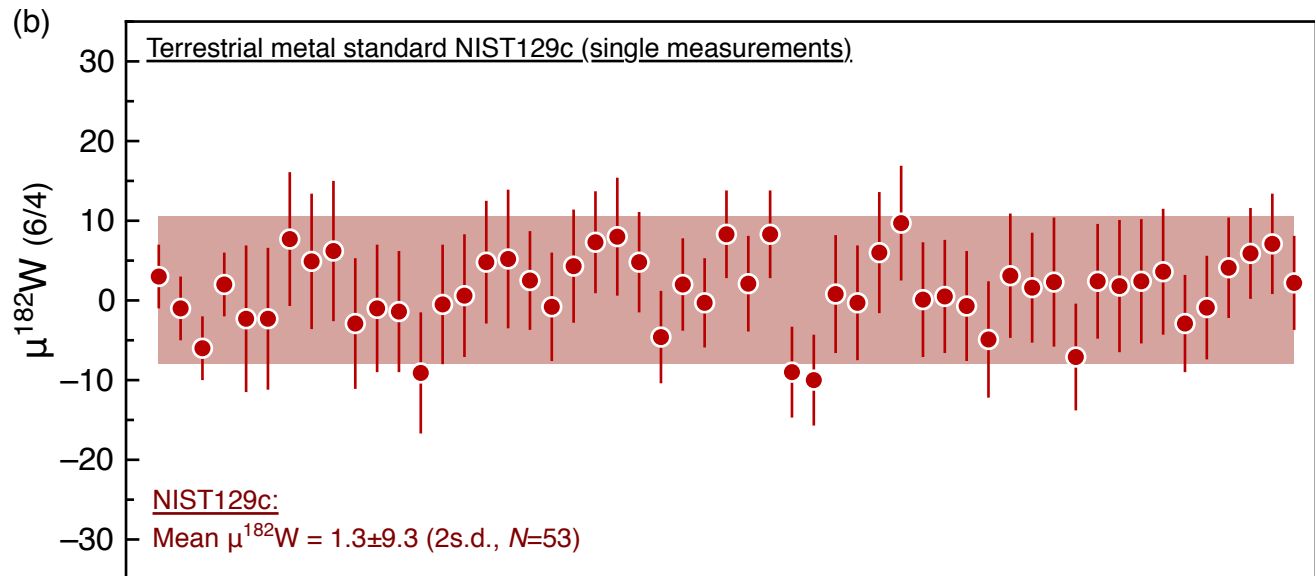
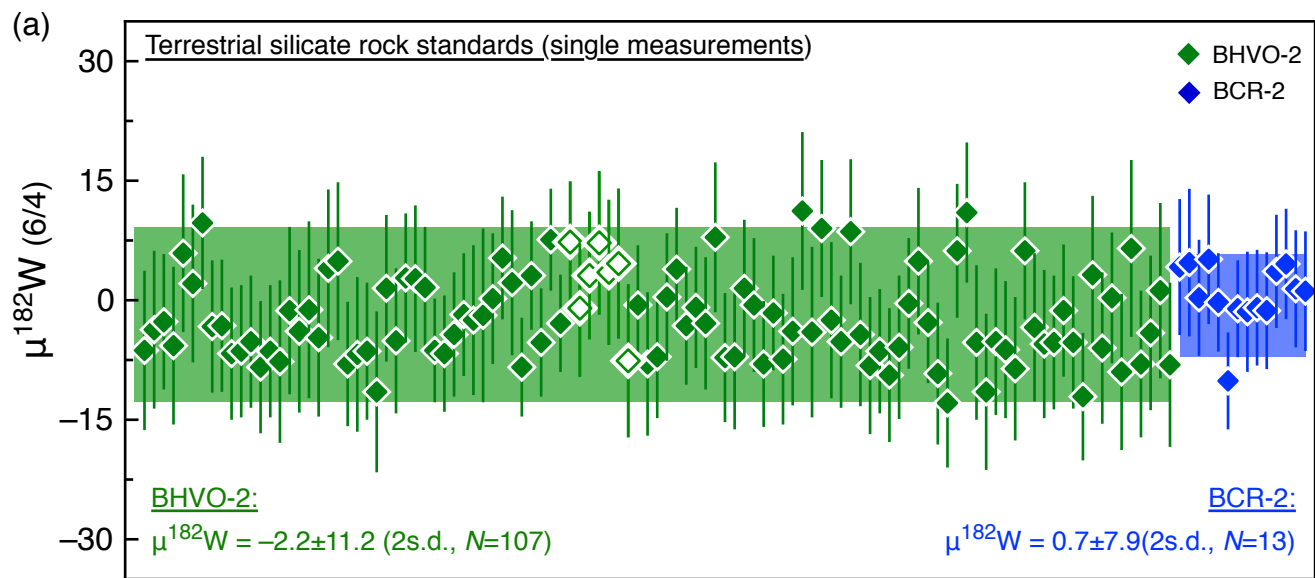
563

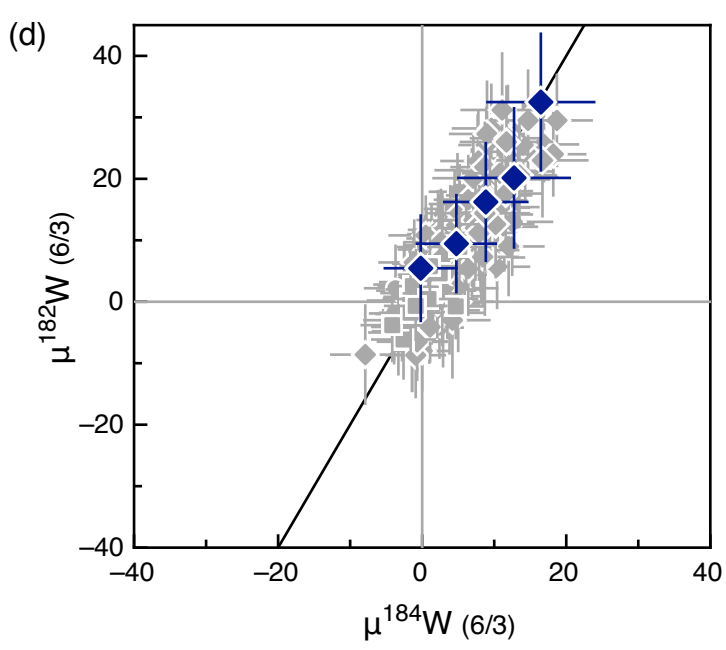
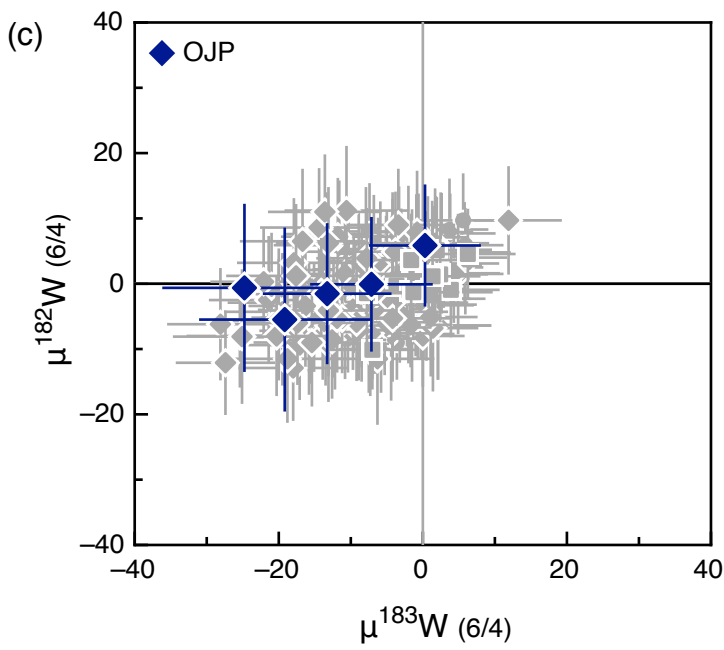
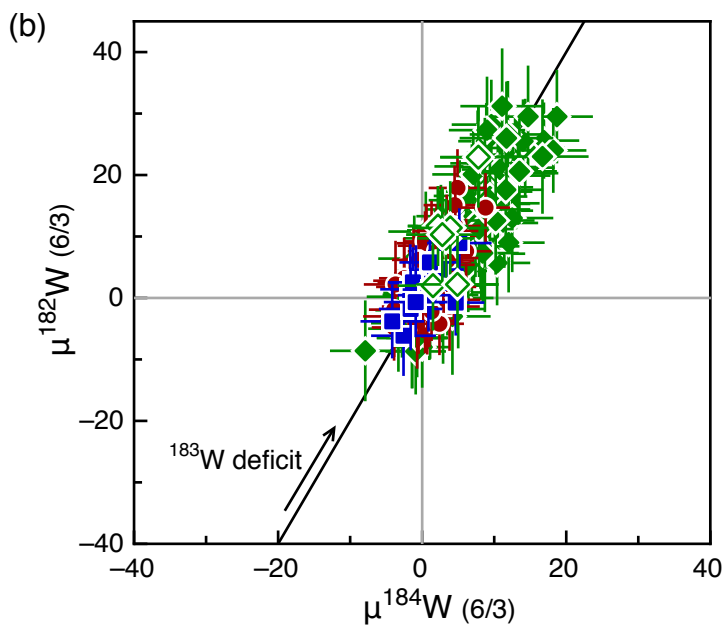
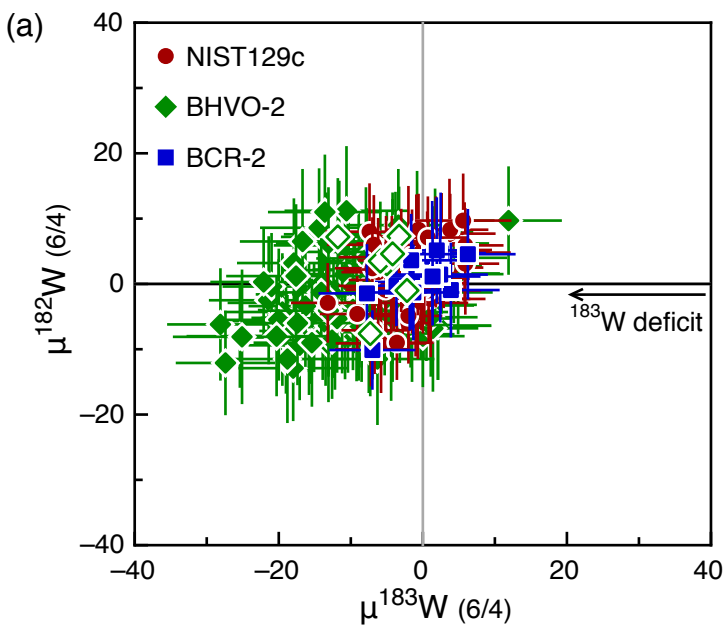
564 **Fig. 5:** Compilation of  $\mu^{182}\text{W}$  data obtained in recent high-precision W isotope studies. Plotted are  
565 data for samples that were analyzed by at least two laboratories. Error bars denote external  
566 uncertainties ( $2\sigma$ ). Distinguished are W isotope analyses by MC-ICPMS (closed symbols) and by  
567 NTIMS (open symbols). Data sources: (1) Rizo et al., 2016a, (2) Willbold et al., 2011, (3) Mundl et  
568 al. (2017), (4) Dale et al., 2017, (5) Kruijjer et al., 2015, (6) Touboul et al., 2015. The measured  $\mu^{182}\text{W}$   
569 value for the individual Isua sample (SM/GR/98/26) analyzed by Willbold et al. (2011) was corrected  
570 for a small analytical effect on  $^{183}\text{W}$  using its measured  $\mu^{183}\text{W}$  (following the equations reported in  
571 Kruijjer et al., 2012; Cook and Schönbächler, 2016). For BHVO-2 the mean  $\mu^{182}\text{W}$  value of each study  
572 is reported.

573

574 **Fig. 6:** Explanatory diagram of  $\mu^{182}\text{W}$  vs.  $\mu^{183}\text{W}$  illustrating how an analytical  $^{183}\text{W}$  effect can lead  
575 to apparent  $\mu^{182}\text{W}$  excesses following the second order mass bias correction used in NTIMS  
576 measurements.

577





# Quintuple measurements of terrestrial reference materials

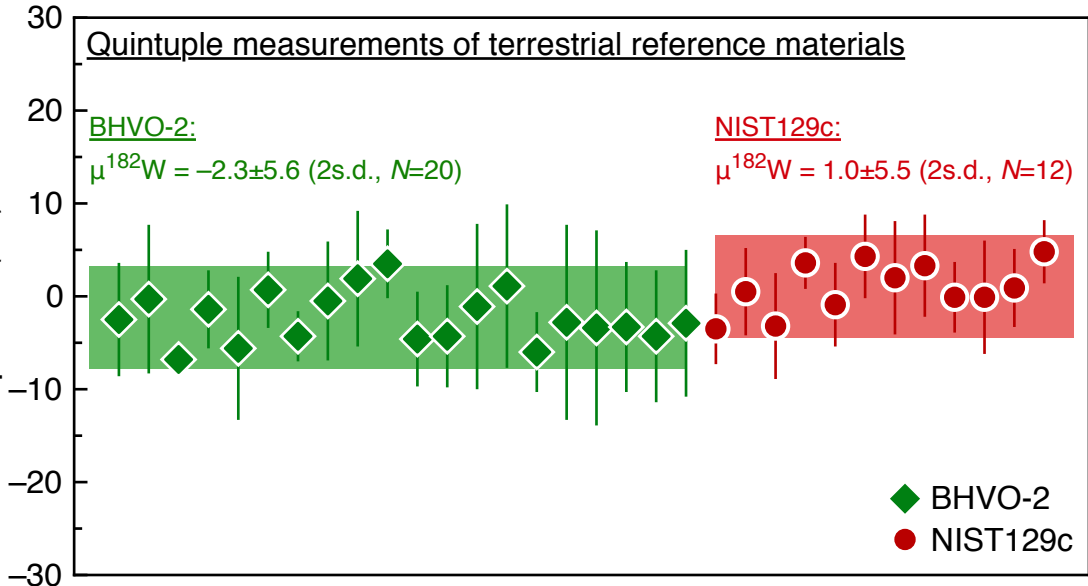
BHVO-2:

$\mu^{182}\text{W} = -2.3 \pm 5.6$  (2s.d.,  $N=20$ )

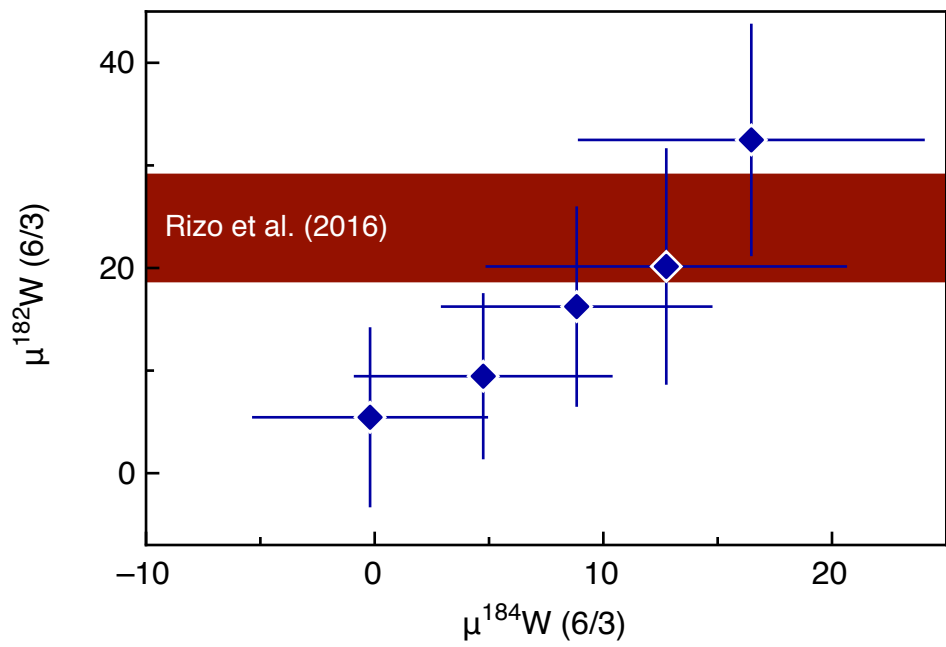
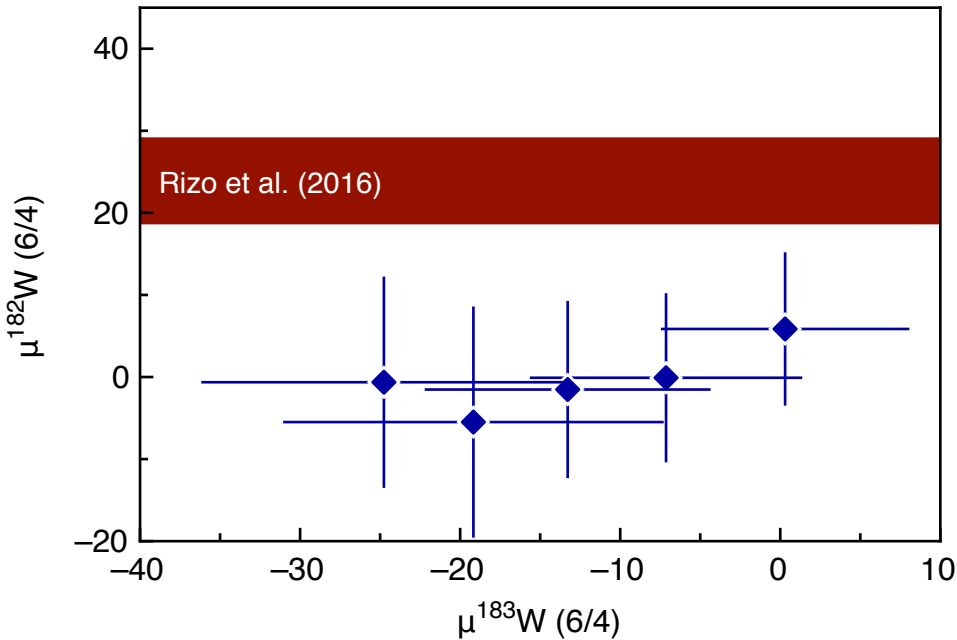
NIST129c:

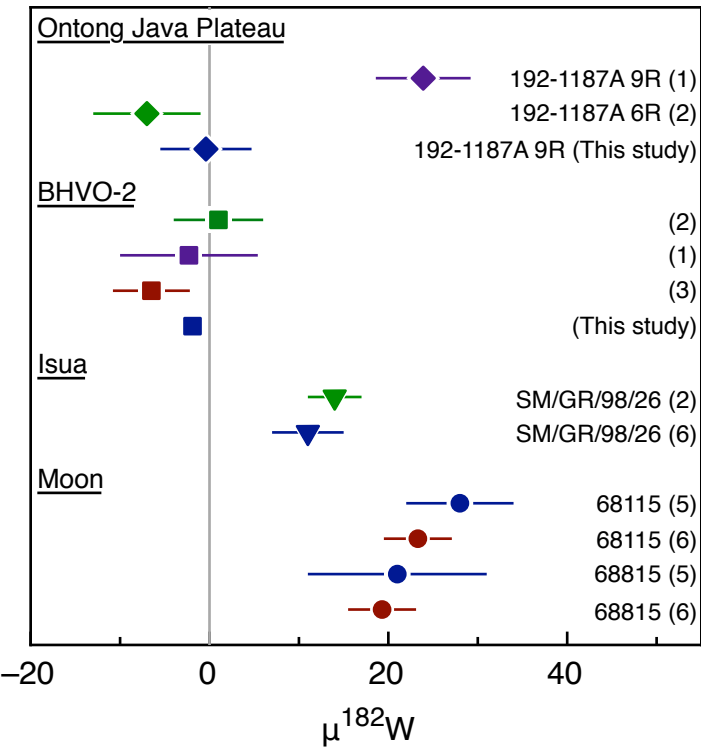
$\mu^{182}\text{W} = 1.0 \pm 5.5$  (2s.d.,  $N=12$ )

$\mu^{182}\text{W}$  (6/4)



- ◆ BHVO-2
- NIST129c





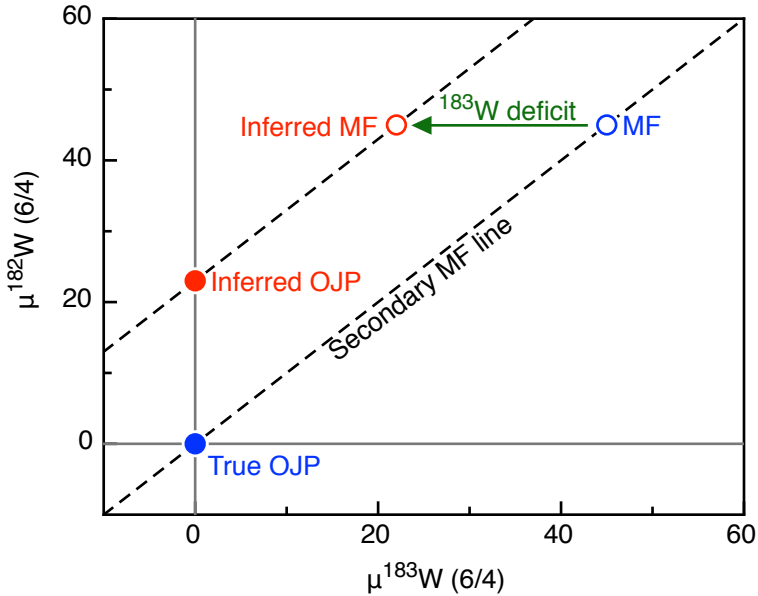


Table 1  
Tungsten isotopic compositions of Ontong Java Plateau drill core samples and reference materials determined by MC-ICPMS.

Sample	ID	Weight (g)	W (ng/g)	Normalized to $^{186}\text{W}/^{184}\text{W} = 0.92767$		Normalized to $^{186}\text{W}/^{183}\text{W} = 1.9859$		$\mu^{182}\text{W}_{\text{corr.}}$ ( $\pm 2\sigma$ ) <sup>a</sup>	
				$\mu^{182}\text{W}_{\text{meas.}}$ ( $\pm 2\sigma$ )	$\mu^{183}\text{W}_{\text{meas.}}$ ( $\pm 2\sigma$ )	$\mu^{182}\text{W}_{\text{meas.}}$ ( $\pm 2\sigma$ )	$\mu^{184}\text{W}_{\text{meas.}}$ ( $\pm 2\sigma$ )		
OJP drill core samples									
192-1187A-009R-04W (118.5-120)	CM01	2.11	17.3	-0.1 $\pm$ 10.3	-7.1 $\pm$ 8.5	9.5 $\pm$ 8.1	4.7 $\pm$ 5.7	0.1 $\pm$ 13.9	
192-1187A-009R-04W (118.5-120)	CN01A	1.27	17.3	5.9 $\pm$ 9.3	0.3 $\pm$ 7.8	5.4 $\pm$ 8.8	-0.2 $\pm$ 5.2	5.8 $\pm$ 13.5	
192-1187A-009R-04W (118.5-120)	CN01BC	2.08	13.4	-5.5 $\pm$ 14.1	-19.2 $\pm$ 11.9	20.1 $\pm$ 11.5	12.8 $\pm$ 7.9	-4.9 $\pm$ 19.6	
192-1187A-009R-04W (15-17)	CM02	2.08	16.2	-1.5 $\pm$ 10.8	-13.3 $\pm$ 8.9	16.2 $\pm$ 9.8	8.8 $\pm$ 5.9	-1.1 $\pm$ 15.4	
192-1187A-009R-04W (15-17)	CN02AB	1.89	15.6	-0.6 $\pm$ 12.9	-24.8 $\pm$ 11.4	32.5 $\pm$ 11.3	16.5 $\pm$ 7.6	0.2 $\pm$ 18.9	
<b>192-1187A-009R-04W</b>		<b>Mean (N=5)</b>	$\pm 2$ s.d.	<b>-0.4 <math>\pm</math> 8.2</b>	-12.8 $\pm$ 19.7	16.8 $\pm$ 21.0	8.5 $\pm$ 13.1	<b>0.0 <math>\pm</math> 7.7</b>	
			$\pm 95\%$ conf.	<b><math>\pm 5.1</math></b>	$\pm 12.2$	$\pm 13.0$	$\pm 8.1$	<b>0.0 <math>\pm</math> 4.8</b>	
Geological reference materials (Mean values)									
BHVO-2		Mean (N=107)	$\pm 2$ s.d.	-2.2 $\pm$ 11.2	-9.7 $\pm$ 15.6	10.9 $\pm$ 19.6	6.5 $\pm$ 10.4	-1.8 $\pm$ 11.2	
BCR-2		Mean (N=13)	$\pm 2$ s.d.	0.7 $\pm$ 7.9	-0.4 $\pm$ 7.9	1.2 $\pm$ 7.7	0.2 $\pm$ 5.3	0.7 $\pm$ 7.8	
NIST 129c		Mean (N=53)	$\pm 2$ s.d.	1.3 $\pm$ 9.3	-1.8 $\pm$ 8.0	3.7 $\pm$ 10.6	1.2 $\pm$ 5.4	1.3 $\pm$ 9.2	

Each analysis represents a single W isotope measurement (200 cycles). Uncertainties on measured  $\mu^i\text{W}$  values of OJP samples (subscript 'meas.') are two standard errors (2s.e.) obtained from internal run statistics.

<sup>a</sup>  $\mu^{182}\text{W}_{\text{corr.}}$ : Corrected for an analytical effect on  $^{183}\text{W}$  according to  $\mu^{182}\text{W}_{\text{corr.}} = \mu^{184}\text{W}_{\text{meas.}} - 1.962 \times \mu^{184}\text{W}_{\text{meas.}}$  (Cook and Schönbacher, 2016; Kruijer et al., 2012).

The added uncertainty induced by this correction is propagated in the reported uncertainties of corrected  $\mu^i\text{W}$  values.